

# CROSS-SECTION OF THE ${}^{\text{nat}}\text{Ni}(\gamma, \text{pxn}){}^{58}\text{Co}$ REACTION AT THE BREMSSTRAHLUNG END-POINT ENERGY OF 35...94 MeV

*I.S. Timchenko*<sup>1,2</sup>, *O.S. Deiev*<sup>1</sup>, *S.M. Olejnik*<sup>1</sup>, *S.M. Potin*<sup>1</sup>,  
*V.A. Kushnir*<sup>1</sup>, *V.V. Mytrochenko*<sup>1</sup>, *S.A. Perezhogin*<sup>1</sup>, *A. Herzán*<sup>2</sup>  
<sup>1</sup>*NSC "Kharkiv Institute of Physics and Technology", Kharkiv, Ukraine;*  
<sup>2</sup>*Institute of Physics, Slovak Academy of Sciences,*  
*SK-84511 Bratislava, Slovakia*

Production of the  ${}^{58}\text{Co}$  nuclei on  ${}^{\text{nat}}\text{Ni}$  in photonuclear reactions using bremsstrahlung irradiation with end-point energy  $E_{\gamma\text{max}}$  between 35 and 94 MeV has been studied. The experiment was performed at the electron linear accelerator LUE-40 NSC KIPT using the methods of  $\gamma$ -activation and off-line  $\gamma$ -ray spectroscopy. The experimental flux-averaged cross-sections  $\langle\sigma(E_{\gamma\text{max}})\rangle$  were determined and compared with the literature data. The theoretical flux-averaged cross-sections  $\langle\sigma(E_{\gamma\text{max}})\rangle_{\text{th}}$  for the production of  ${}^{58\text{m,g}}\text{Co}$  and  ${}^{58}\text{Co}$  were estimated using the cross-section values  $\sigma(E)$  from the TALYS1.96 code for different level density models and gamma strength functions.

## INTRODUCTION

Nuclear reactions are the central tool for studying the structure of nuclei. Their importance is constantly growing. Experimental data from photonuclear reactions are necessary for studying the fundamental processes occurring in nuclear matter and are necessary for creating theoretical models of the atomic nucleus. For example, this is the study of the giant dipole resonance (GDR), the mechanisms of its excitation and decay, including the competition between statistical and direct processes in the decay channels, the configurational and isospin splitting of GDR, the exhaustion of the sum rule, etc.

Photonuclear reaction cross-sections are used in various applications of science and technology, primarily in the production of isotopes and in nuclear medicine, in the development of modern models of reactors and subcritical systems controlled by accelerators, the calculation of radiation protection systems, the design of intensive neutron sources, the disposal of long-lived radioactive waste products, etc.

The photonuclear cross-sections on  ${}^{\text{nat}}\text{Ni}$  are important because the reaction products, nickel and cobalt, are of practical interest as an important structural and surface material, which is often used in structural materials for accelerator and nuclear technology [1-3], in medicine [4], as calibration sources [5], etc.

Experimental data on cross-sections for photonuclear reactions on nickel at energies in the range of 12...40 MeV were obtained in a number of studies, e.g. [6-8]. At higher energies, the study of cross-sections on natural nickel using electron bremsstrahlung was performed in [9, 10]. The flux-averaged cross-sections of  ${}^{\text{nat}}\text{Ni}(\gamma, \text{pxn}){}^{55-58}\text{Co}$  reactions were determined in these studies using the  $\gamma$ -activation technique at bremsstrahlung end-point energies of 55...65 MeV [9] and 65...75 MeV [10].

This work is a continuation of our experimental studies of photonuclear reactions on natural nickel. Previously, we obtained cross-sections for the reactions  ${}^{\text{nat}}\text{Ni}(\gamma, \text{xn}){}^{56,57}\text{Ni}$  [12] and  ${}^{\text{nat}}\text{Ni}(\gamma, \text{pxn}){}^{55,56,57}\text{Co}$  [13].

In this work, results of the experimental study of the  ${}^{58}\text{Co}$  production in photonuclear reactions on natural nickel measured using bremsstrahlung spectra of gamma photons with end-point energy  $E_{\gamma\text{max}}$  between 35

and 94 MeV are presented. The obtained data are compared both with the theoretical calculation performed using partial cross-sections  $\sigma(E)$  from the TALYS1.96 code [11], and with the experimental data available in the literature [9, 10].

## 1. EXPERIMENTAL PROCEDURE

An experiment to study the photoproduction of  ${}^{58\text{m,g}}\text{Co}$  nuclei on  ${}^{\text{nat}}\text{Ni}$  was carried out using the bremsstrahlung beam delivered by the LUE-40 electron linear accelerator of the National Science Center of the Kharkov Institute of Physics and Technology using the induced  $\gamma$ -activity method and offline  $\gamma$ -ray spectroscopy. This technique has been described in many studies of photonuclear reactions, e.g. [14-17]. The schematic block diagram of the experiment is presented in Fig. 1.

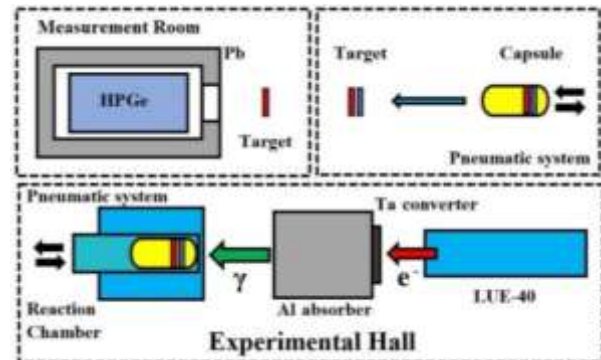


*Fig. 1. Schematic block diagram of the experiment. The upper part shows the measurement room, where the irradiated target (red color) and the target-monitor (blue color) are extracted from the capsule and are arranged by turn before the HPGe detector for induced  $\gamma$ -activity measurements. The lower part shows the accelerator LUE-40, the Ta converter, Al absorber, exposure reaction chamber*

For investigation of photoproduction of  ${}^{58}\text{Co}$ , natural Ni and Mo targets of diameter 8 mm and the masses, respectively,  $\sim 80$  and  $\sim 60$  mg, were used in the experiment. The isotopic composition of nickel is a mixture of five stable isotopes with an isotopic abundance:  ${}^{58}\text{Ni}$  – 0.68077,  ${}^{60}\text{Ni}$  – 0.26223,  ${}^{61}\text{Ni}$  – 0.0114,  ${}^{62}\text{Ni}$  – 0.03634,  ${}^{64}\text{Ni}$  – 0.00926. For  ${}^{100}\text{Mo}$  in

our calculations, we have used the percentage value of isotope abundance equal to 9.63% [18]. The admixture of other elements in the targets did not exceed 0.1% by weight. The time of irradiation  $t_{\text{irr}}$  and the time of residual  $\gamma$ -activity spectrum measurement  $t_{\text{meas}}$  were 30 min for each energy  $E_{\gamma\text{max}}$  value.

The bremsstrahlung spectra of electrons were calculated using the GEANT4.9.2 code [18], where the real geometry of the experimental setup was taken into account, as well as the spatial and energy distributions of the electron beam. In addition, the bremsstrahlung gamma fluxes were monitored by the  $^{100}\text{Mo}(\gamma, n)^{99}\text{Mo}$  reaction yield. Description of the monitoring procedure can be found in [19, 20].

To process the spectra and estimate the full absorption peak areas  $\Delta A$ , the program InterSpec V.1.0.12 [21] was used. Nuclear spectroscopic data required to study the  $^{\text{nat}}\text{Ni}(\gamma, \text{pxn})^{58}\text{Co}$  reaction were adopted from [22].

The  $^{58}\text{Co}$  nucleus in reactions on  $^{\text{nat}}\text{Ni}$  can be formed in the isomeric  $m$  and ground  $g$  states. However, it is impossible to measure the cross-section of the  $^{58m}\text{Co}$  nucleus formation since the excitation energy of the isomeric state is only 24.89 keV, and the corresponding gamma transition has a low intensity of 0.039% [22]. As a result of the internal transition (100%), the isomeric state decays to a ground state with a half-life  $T_{1/2} = (9.10 \pm 0.09)$  h. In the experiment, the cooling time was more than  $t_{\text{cool}} = 32$  d, sufficient for the complete decay of the metastable state into the ground state. Thus, we measure the total cross-section of the formation of the  $^{58}\text{Co}$  nucleus on natural nickel.

## 2. RESULTS AND DISCUSSION

TALYS [11] is a computational code based on modern concepts of nuclear interactions, which provides simulation of nuclear reactions over a wide range of energies and atomic masses.

Here, various parametrizations reflecting the use of a set of level density models ( $LD$ ) and gamma-strength functions ( $GSF$ ) were considered to give the theoretical cross-section values  $\sigma(E)$  for the photoproduction reactions of the  $^{58}\text{Co}$  nucleus on stable isotopes of  $^{\text{nat}}\text{Ni}$ .

Fig. 2 shows the calculated cross-sections  $\sigma(E)$  of the formation of the  $^{58}\text{Co}$  nucleus in photonuclear reactions on stable isotopes of  $^{\text{nat}}\text{Ni}$ , taking into account the isotopic abundance. The cross-section of formation on  $^{\text{nat}}\text{Ni}$  is the sum of the cross-sections on 4 from 5 stable isotopes of nickel. It is evident, that the main contribution to the cross-section of  $^{58}\text{Co}$  formation comes from the reaction on  $^{60}\text{Ni}$ .

In Fig. 3, the calculated cross-sections  $\sigma(E)$  of the formation of the  $^{58}\text{Co}$  nucleus in metastable and ground states were shown. One can see that ratio of meta/ground is approximately 20%. As a rule, the accuracy of the calculation of the metastable cross-section is low, however, since this contribution is small, the total cross-section for this reaction will be calculated with good reliability.

Different  $LD$  (1 - 6) and  $GSF$  (1 - 9) parameters combinations lead to altogether 54 different theoretical  $\sigma(E)$  values. The minimum value was obtained for the

case of a combination of parameters  $LD6$  and  $GSF2$ , and the maximum –  $LD3$  and  $GSF7$ .

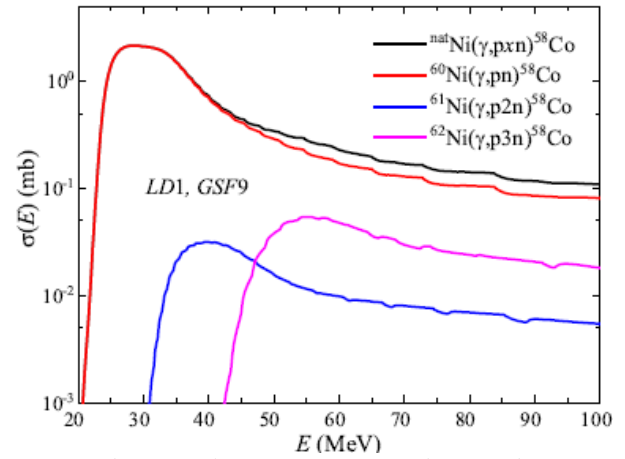


Fig. 2. Theoretical cross-sections of photoproduction of the  $^{58}\text{Co}$  nucleus on nickel isotopes (taking into account the isotopic abundance) and  $^{\text{nat}}\text{Ni}$ . Calculated with the TALYS1.96 code for the default parameters –  $LD1$  and  $GSF9$

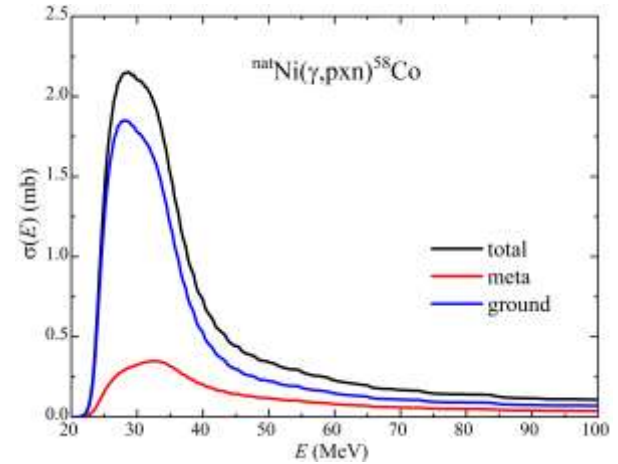


Fig. 3. Theoretical cross-sections  $\sigma(E)$  for the  $^{\text{nat}}\text{Ni}(\gamma, \text{pxn})^{58}\text{Co}$  reaction with production of  $^{58}\text{Co}$  in metastable, ground states and total cross-sections. Calculated with the TALYS1.96 code for the default parameters –  $LD1$  and  $GSF9$

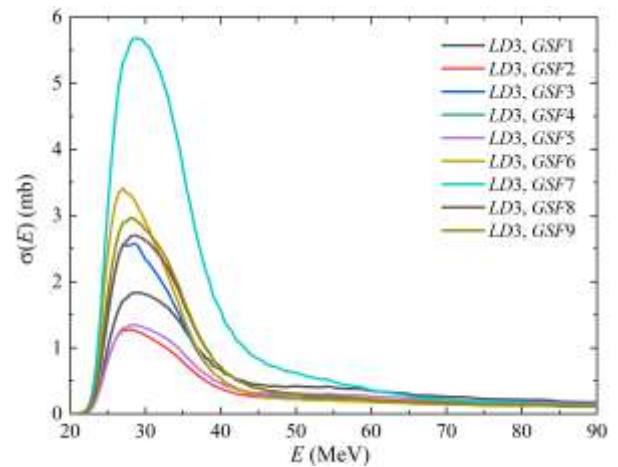


Fig. 4. Cross-sections  $\sigma(E)$  for the  $^{\text{nat}}\text{Ni}(\gamma, \text{pxn})^{58}\text{Co}$  reaction calculated with the TALYS1.96 code for  $LD3$  and  $GSF$  (1 – 9)

The observed difference for these combinations reaches ~8 times. A difference in the position of the cross-section maxima is also observed. Figure 4, as an example, shows the calculation results for parameters LD3 and GSF 1-9.

In experiments on the bremsstrahlung beam, it is possible to determine the value of the flux-averaged cross-section  $\langle\sigma(E_{\gamma\max})\rangle$  of the reaction under study. This value is calculated using the following formula:

$$\langle\sigma(E_{\gamma\max})\rangle = \frac{\lambda\Delta A}{\varepsilon N_n I_\gamma \Phi(E_{\gamma\max}) (1 - e^{-\lambda t_{\text{irr}}}) e^{-\lambda t_{\text{cool}}} (1 - e^{-\lambda t_{\text{meas}}})}, \quad (1)$$

where  $\Delta A$  is the number of counts of  $\gamma$ -quanta in the full absorption peak at the energy of  $\gamma$ -ray transition associated with the decay of the nucleus,  $\lambda$  is the decay constant (in  $\text{s}^{-1}$ ),  $N_n$  is the number of target nuclei,  $I_\gamma$  is the intensity of the analyzed  $\gamma$ -ray transition,  $\varepsilon$  is the absolute detection efficiency for the analyzed  $\gamma$ -quanta energy,  $t_{\text{irr}}$ ,  $t_{\text{cool}}$  and  $t_{\text{meas}}$  are the irradiation time, cooling time and measurement time, respectively (in seconds).

$\Phi(E_{\gamma\max}) = \int_{E_{\text{thr}}^{\min}}^{E_{\gamma\max}} W(E, E_{\gamma\max}) dE$  the integrated flux of bremsstrahlung quanta in the energy range from the reaction threshold  $E_{\text{thr}}^{\min}$  up to  $E_{\gamma\max}$ .

For comparison with the experimental average cross-sections, the theoretical values of  $\langle\sigma(E_{\gamma\max})\rangle$  were calculated using the cross-sections  $\sigma(E)$  from the TALYS1.96 code and the bremsstrahlung  $\gamma$ -flux  $W(E, E_{\gamma\max})$  calculated in GEANT4.9.2 using the formula:

$$\langle\sigma(E_{\gamma\max})\rangle = \frac{\int_{E_{\text{thr}}^{\min}}^{E_{\gamma\max}} \sigma(E) W(E, E_{\gamma\max}) dE}{\int_{E_{\text{thr}}^{\min}}^{E_{\gamma\max}} W(E, E_{\gamma\max}) dE}. \quad (2)$$

The calculation of the experimental cross-sections  $\langle\sigma(E_{\gamma\max})\rangle$  was performed according to formula (1), using the gamma-quantum flux from the reaction threshold with the minimum threshold energy  $E_{\text{thr}}^{\min} = 19.99$  MeV. For the theoretical calculation by the formula (2) also used the value  $E_{\text{thr}}^{\min}$ . This threshold corresponds to the reaction of formation of  $^{58}\text{Co}$  on  $^{60}\text{Ni}$ .

To obtain the experimental values of the average cross-sections  $\langle\sigma(E_{\gamma\max})\rangle$  for the  $^{nat}\text{Ni}(\gamma, \text{pxn})^{58}\text{Co}$  reaction, the 810.76 keV transition with intensity of 99.45% was used. However, there is a  $\gamma$ -ray transition with a similar energy, 811.85 keV, corresponding to the decay of the  $^{56}\text{Ni}$  nucleus, which is formed in the  $^{nat}\text{Ni}(\gamma, \text{xn})$  reactions. This 811.85 keV  $\gamma$  ray contributed to the measured full absorption peak at 810.76 keV, artificially increasing its intensity. To calculate the magnitude of this contribution, the induced activity of the  $^{56}\text{Ni}$  nucleus was measured at the 158.38 keV  $\gamma$ -ray transition and recalculated to the expected activity for 811.85 keV  $\gamma$ -ray transition, taking into account the intensities  $I_\gamma(158.38) = 98.8\%$  and  $I_\gamma(811.85) = 86.0\%$ , and the detector registration efficiency  $\varepsilon$ .

The experimental flux-averaged cross-sections  $\langle\sigma(E_{\gamma\max})\rangle$  obtained in the experiment for the  $^{nat}\text{Ni}(\gamma, \text{pxn})^{58}\text{Co}$  reaction are shown in Fig. 5.

Experimental average cross-sections  $\langle\sigma(E_{\gamma\max})\rangle$  for photonuclear reactions on  $^{nat}\text{Ni}$  with the formation of cobalt isotopes  $^{55-58}\text{Co}$  were obtained in [9,10]. It is important to highlight that the work of Naik et al. [10] involved an analysis of data for the reaction  $^{nat}\text{Ni}(\gamma, \text{pxn})^{58}\text{Co}$ , as presented in the earlier work of Zaman et al. [9]. In this analysis, a correction was made to account for the contribution from the activity of the  $^{56}\text{Ni}$  nucleus for the  $\gamma$ -ray transition with an energy of  $E_\gamma = 810.78$  keV. As can be seen from Fig. 5, the magnitude of this contribution can have a significant impact on the cross-sections  $\langle\sigma(E_{\gamma\max})\rangle$  for the  $^{nat}\text{Ni}(\gamma, \text{pxn})^{58}\text{Co}$ .

Our previously obtained experimental data for the reactions  $^{nat}\text{Ni}(\gamma, \text{pxn})^{55,56,57}\text{Co}$  [13] are in good agreement with the results of Naik et al. [10]. At the same time, the cross-section of the reaction  $^{nat}\text{Ni}(\gamma, \text{pxn})$  with the formation of  $^{58}\text{Co}$  nuclei significantly exceeds the results reported in [9, 10], see Fig. 5.

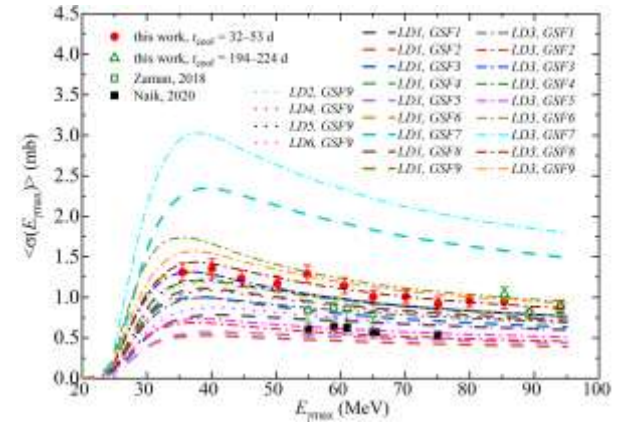


Fig. 5. The bremsstrahlung flux-averaged cross-section  $\langle\sigma(E_{\gamma\max})\rangle$  for the reactions  $^{nat}\text{Ni}(\gamma, \text{pxn})^{58}\text{Co}$ . The experimental data: red circles and green triangles – our data for  $t_{\text{cool}} = 32-53$  and  $194-224$  days, respectively; black empty and full circles – data from Zaman 2018 [9] and Naik 2020 [10], respectively. The theoretical curves are denoted by different colors (see figure for explanation)

### 3. CONCLUSIONS

The total flux-averaged cross-section  $\langle\sigma(E_{\gamma\max})\rangle$  for the  $^{nat}\text{Ni}(\gamma, \text{pxn})^{58}\text{Co}$  reaction has been measured in the range of bremsstrahlung end-point energies  $E_{\gamma\max} = 35 \dots 94$  MeV. The obtained  $\langle\sigma(E_{\gamma\max})\rangle$  were compared with experimental data from the literature and theoretical estimates. The theoretical values of  $\langle\sigma(E_{\gamma\max})\rangle_{\text{th}}$  were calculated using the partial cross-sections  $\sigma(E)$  from the TALYS1.96 code for different level density models LD 1-6 and photon strength functions GSF 1-9. A large number of theoretical estimates with close results makes it difficult to choose the optimal curve for describing the experimental data. The comparison showed that the measured flux-averaged cross-sections for the  $^{nat}\text{Ni}(\gamma, \text{pxn})^{58}\text{Co}$  reaction are in satisfactory agreement with several calculation estimates within the TALYS1.96 code (LD1 + GSF 6, 9; LD3 + GSF 3, 8, 9).

This work was supported by the Slovak Research and Development Agency under No. APVV-20-0532

and the Slovak grant agency VEGA (Contract No. 2/0175/24). Funded by the EU NextGenerationEU through the Recovery and Resilience Plan for Slovakia under the project No. 09I03-03-V01-00069.

## REFERENCES

1. S. Takacs, F. Tarkanyi, B. Kiraly, A. Hermanne, M. Sonck. Evaluated activation cross-sections of longer-lived radionuclides produced by deuteron induced reactions on natural nickel // *Nucl. Instrum. Methods B*. 2007, 260, 495. dx.doi.org/10.1016/j.nimb.2006.11.136.
2. K.L. Murty, I. Charit. Structural materials for Gen-IV nuclear reactors: Challenges and opportunities // *J. Nucl. Mater.* 2008, 383, 189. dx.doi.org/10.1016/j.jnucmat.2008.08.044.
3. U. Fischer, P. Batistoni, E. Cheng, et al. Nuclear Data for Fusion Energy Technologies: Requests, Status and Development Needs // *AIP Conf. Proc.* 2005, 769, 1478. dx.doi.org/10.1063/1.1945284.
4. S. Spellerberg, P. Reimer, G. Blessing, et al. Production of  $^{55}\text{Co}$  and  $^{57}\text{Co}$  via proton induced reactions on highly enriched  $^{58}\text{Ni}$  // *Appl. Radiat. Isot.* 1998, 49, 1519. dx.doi.org/10.1016/S0969-8043(97)10119-1.
5. H. Miyahara, A. Yoshida, N. Ishikawa, Ch. Mori // *Appl. Radiat. Isot.* 1998, 49, 1159. [http://dx.doi.org/10.1016/S0969-8043\(97\)10038-0](http://dx.doi.org/10.1016/S0969-8043(97)10038-0).
6. K. Min, T.A. White // *Phys. Rev. Lett.* 21 1968, 1200. <http://dx.doi.org/10.1103/PhysRevLett.21.1200>.
7. D.G. Owen, E.G. Muirhead, B.M. Spicer // *Nucl. Phys. A*. 1970,140, 523. [http://dx.doi.org/10.1016/0375-9474\(70\)90577-4](http://dx.doi.org/10.1016/0375-9474(70)90577-4).
8. B.I. Goryachev, B.S. Ishkhanov, I.M. Kapitonov, I.M. Piskarev, V.G. Shevchenko, O.P. Shevchenko // *JETF Lett.* 1968, 8, 46.
9. M. Zaman, G. Kim, H. Naik, et al. Flux weighted average cross-sections of  $^{nat}\text{Ni}(\gamma,x)$  reactions with the bremsstrahlung end-point energies of 55, 59, 61 and 65 MeV // *Nucl. Phys. A* 2018, 978, 173. dx.doi.org/10.1016/j.nuclphysa.2018.07.017.
10. H. Naik, G. Kim, Th.H. Nguyen, K. Kim, S.G. Shin, Y. Kye, M.H. Cho, J. Radioanal. Nucl. Chem. 2020, 324, 837. <http://dx.doi.org/10.1007/s10967-020-07105-9>.
11. A.J. Koning, D. Rochman, J. Sublet, N. Dzysiuk, M. Fleming, S. van der Marck // *Nucl. Data Sheets*. 155 2019 1. <http://dx.doi.org/10.1016/j.nds.2019.01.002>.
12. O.S. Deiev, I.S. Timchenko, S.N. Olejnik, et al. Photonuclear reactions  $^{nat}\text{Ni}(\gamma,xn)^{57}\text{Ni}$  and  $^{nat}\text{Ni}(\gamma,xn)^{56}\text{Ni}$  in the energy range  $E_{\gamma\text{max}} = 35\dots94$  MeV // *Nuclear Physics*. 2022, A 1028 122542. doi:10.1016/j.nuclphysa.2022.122542.
13. I.S. Timchenko, O.S. Deiev, S.M. Olejnik, et al. Photoproduction of the  $^{55-57}\text{Co}$  nuclei on  $^{nat}\text{Ni}$  at the bremsstrahlung end-point energy of 35–94 MeV // *Atomic Data and Nuclear Data Tables*. 2024, 160, 101674. doi.org/10.1016/j.adt.2024.101674.
14. A.N. Vodin, O.S. Deiev, I.S. Timchenko, et al. Photoneutron cross-sections for the reactions  $^{181}\text{Ta}(\gamma,xn; x = 1-8)^{181-x}\text{Ta}$  at  $E_{\gamma\text{max}} = 80-95$  MeV // *Eur. Phys. J. A*. 2021, 57, 208. dx.doi.org/10.1140/epja/s10050-021-00484-x, arXiv:2103.09859.
15. O.S. Deiev, I.S. Timchenko, S.N. Olejnik, et al. Isomeric ratio of the  $^{181}\text{Ta}(\gamma,3n)^{178\text{m,g}}\text{Ta}$  reaction products at energy  $E_{\gamma\text{max}}$  up to 95 MeV // *Chinese Phys.* 2022, C 46, 014001. dx.doi.org/10.1088/1674-1137/ac2a95, arXiv:2108.01635.
16. O.S. Deiev, I.S. Timchenko, S.M. Olejnik, et al. Cross-sections of photonuclear reactions  $^{65}\text{Cu}(\gamma,n)^{64}\text{Cu}$  and  $^{63}\text{Cu}(\gamma,xn)^{63-x}\text{Cu}$  in the energy range  $E_{\gamma\text{max}} = 35-94$  MeV // *Chinese Physics*. 2022,C46, 124001. dx.doi.org/10.1088/1674-1137/ac878a.
17. O.S. Deiev, I.S. Timchenko, S.M. Olejnik, et al. Cross-sections for the  $^{27}\text{Al}(\gamma,x)^{22}\text{Na}$  multichannel reaction with the 28.3 MeV difference of reaction thresholds // *Chinese Phys.* 2022, C46, 064002. dx.doi.org/10.1088/1674-1137/ac5733
18. S. Agostinelli, J. Allison, K. Amako, et al. // *Nucl. Instrum. Meth. Phys. Res.* 2003, A 506, 250. [http://dx.doi.org/10.1016/S0168-9002\(03\)01368-8](http://dx.doi.org/10.1016/S0168-9002(03)01368-8), <http://GEANT4.9.2.web.cern.ch/GEANT4.9.2/>.
19. A.N. Vodin, O.S. Deiev, I.S. Timchenko, et al. Cross-sections for photonuclear reactions  $^{93}\text{Nb}(\gamma,n)^{92\text{m}}\text{Nb}$  and  $^{93}\text{Nb}(\gamma,n)^{92\text{l}}\text{Nb}$  at boundary energies of bremsstrahlung  $\gamma$ -energies  $E_{\gamma\text{max}} = 36\dots91$  MeV // *Probl. Atom. Sci. Tech.* 2020, v. 3, p. 148.
20. A.N. Vodin, O.S. Deiev, V.Yu. Korda, I.S. Timchenko, et al. Photoneutron reactions on  $^{93}\text{Nb}$  at  $E_{\gamma\text{max}} = 33-93$  MeV // *Nucl. Phys.* 2021, A1014, p. 122248. doi.org/10.1016/j.nuclphysa.2021.122248.
21. InterSpec – spectral radiation analysis software (v. 1.0.12) // <https://github.com/sandialabs/InterSpec>.
22. Live Chart of Nuclides – nuclear structure and decay data // <https://www.nds.iaea.org/relnsd/vcharthtml/VChartHTML.html>.